Quasifission process in a transport model for a dinuclear system

A. Diaz-Torres,[1] G. G. Adamian,[1,2,3] N. V. Antonenko,[1,2] and W. Scheid[1]
[1]*Institut für Theoretische Physik der Justus-Liebig-Universität, D-35392 Giessen, Germany*
[2]*Joint Institute for Nuclear Research, RU-141980 Dubna, Russia*
[3]*Institute of Nuclear Physics, 702132 Tashkent, Uzbekistan*
(Received 15 December 2000; published 25 June 2001)

A new method is suggested for calculating the charge and mass distributions of quasifission products. The quasifission is treated within a transport model describing the evolution of a dinuclear system in charge (mass) asymmetry and the decay of this system along the internuclear distance. The calculated yields of these products are in agreement with recent experimental data for the hot fusion reactions leading to superheavy nuclei. The quasifission distributions in cold Pb-based fusion reactions are predicted.

DOI: 10.1103/PhysRevC.64.024604 PACS number(s): 25.70.Jj, 24.10.−i, 24.60.−k, 27.90.+b

I. INTRODUCTION

The experimental evaporation residue cross sections in cold (^{208}Pb- and ^{209}Bi-based) and hot (actinide-based) fusion reactions leading to the production of heavy and superheavy nuclei [1–3] can be well reproduced in the dinuclear system (DNS) model of fusion [4–9]. In order to support and to prove the DNS mechanism of fusion, it is very crucial and important to describe also other experimental observables, like mass and charge distributions of the quasifission products which accompany the fusion process. The aim of this paper is to describe the quasifission yields inside the DNS model.

In the quasifission process one finds large mass rearrangements between the interacting heavy ions occurring on a short time scale [10–12]. The experimental signatures of this process are the large widths of mass distributions and enhanced angular anisotropy, incompatible with compound nucleus fission. The quasifission conceptually bridges the gap [13] between deep-inelastic collisions, where the reaction partners get into close contact to exchange many particles without altering their average mass and charge [14], and the complete fusion process where the reaction partners lose their identity after forming the compound nucleus [11]. As shown in [4–9,15,16], quasifission and fusion have the common property to be described as an evolution of the DNS which is formed in the entrance channel during the capture stage of the reaction, after dissipation of the kinetic energy of the collision. One can assume that the decay of the DNS which evolves in mass asymmetry coordinate predestines the charge and mass distributions of the quasifission products.

In the DNS model [5–9] the total quasifission cross section

$$\sigma_{qf}(E_{\mathrm{c.m.}})=\sum_{J=0}\sigma_{cap}(E_{\mathrm{c.m.}},J)[1-P_{CN}(E_{\mathrm{c.m.}},J)] \quad (1)$$

depends on the partial capture cross section σ_{cap} for the transition of the colliding nuclei over the entrance (Coulomb) barrier and on the probability P_{CN} of the compound nucleus formation after the capture. In the first step of a fusion reaction the projectile is captured by the target and a DNS is formed which either evolves into the compound nucleus or decays (quasifission). The partial capture cross section for the transition of the colliding nuclei over the Coulomb barrier with probability $T(E_{\mathrm{c.m.}},J)$ and for the formation of the DNS is given by

$$\sigma_{cap}(E_{\mathrm{c.m.}},J)=\pi\lambda\!\!\!^{-2}(2J+1)T(E_{\mathrm{c.m.}},J), \quad (2)$$

where $\lambda\!\!\!^{-2}=\hbar^2/(2\mu E_{\mathrm{c.m.}})$ is the reduced de Broglie wavelength and μ the reduced mass. The probability of complete fusion $P_{CN}(E_{\mathrm{c.m.}},J)$ depends on the competition between the complete fusion and quasifission. Since in this paper we are interested in reactions with heavy ions which occur near the Coulomb barrier and in partial waves with small J which are typical for fusion and quasifission, only partial waves with angular momenta less than the critical angular momentum contribute to the sum in Eq. (1). Larger values of J correspond to deep inelastic collisions and are not treated here. For small J, the values of $P_{CN}(E_{\mathrm{c.m.}},J)$ are not much different from $P_{CN}(E_{\mathrm{c.m.}},J=0)=P_{CN}(E_{\mathrm{c.m.}})$. Then we can write the quasifission cross section as

$$\sigma_{qf}(E_{\mathrm{c.m.}})\approx[1-P_{CN}(E_{\mathrm{c.m.}})]\sum_{J=0}\sigma_{cap}(E_{\mathrm{c.m.}},J)$$
$$=[1-P_{CN}(E_{\mathrm{c.m.}})]\sigma_{cap}(E_{\mathrm{c.m.}}). \quad (3)$$

The total quasifission cross section can be splitted into the cross sections $\sigma_{qf}(E_{\mathrm{c.m.}},A)$ of the quasifission products with certain mass numbers A, $\sigma_{qf}(E_{\mathrm{c.m.}})=\Sigma_A\sigma_{qf}(E_{\mathrm{c.m.}},A)$.

In spite of an intensive experimental study of the quasifission process, no microscopical model was elaborated for calculating the yields of quasifission products up to now. In Sec. II of this paper such a model is presented. The results of calculations in comparison with experimental data are shown in Sec. III. A short summary is given in Sec. IV.

II. MODEL

A. Evolution of the DNS in charge (mass) asymmetry coordinate

The DNS model [5–9] of fusion assumes that the compound nucleus is reached by a series of transfers of nucleons or small clusters from the light nucleus to the heavier one in

a touching configuration. So, the dynamics of fusion is considered as a diffusion of the DNS in the charge (mass) $Z(A)$ asymmetry coordinate, defined by the charge (mass) number of the light fragment of the DNS. The potential inner barrier B^*_{fus} in the Z (A) coordinate supplies a hindrance for the fusion in the DNS model which well reproduces the existing experimental data for the fusion evaporation residue cross sections.

While the DNS model suggested in Refs. [5–9] allows us to describe the fusion probability P_{CN} and total quasifission cross section σ_{qf}, it has to be modified to calculate the charge (mass) distribution of the quasifission products. We suggest a new variant of the DNS model for the quasifission process where the DNS simultaneously evolves in $Z(A)$ by nucleon transfer between the nuclei and in R by decay into the direction of increasing internuclear distance. A diffusion process leads to the exchange of nucleons between the two touching fragments, thus generating a time-dependent distribution in the charge (mass) asymmetry of the DNS. This process can be described by a master equation [14,17,18] for the probability $P_Z(t)$ to find the DNS at the time t in the configuration with charge numbers Z and $Z_{tot}-Z$, where Z_{tot} is the total charge number of the system. This master-equation is derived from the microscopic treatment [14,19] assuming the validity of the kinetic approach in the DNS and the shorter time for reaching internal equilibrium at fixed Z than the transition time between the states with different Z. The initial DNS with $Z=Z_i$ evolves to a compound nucleus or to the symmetric DNS. The melting of the DNS nuclei to smaller values of the variable R is strongly hindered due to the structural forbiddenness effect [20–25]. The decay in R affects the motion of the system in Z. In order to take the effect of the DNS decay into consideration, we modify the known master-equation for $P_Z(t)$ [14,17,18] as follows:

$$\frac{\partial P_Z(t)}{\partial t}=\Delta^{(-)}_{Z+1}P_{Z+1}(t)+\Delta^{(+)}_{Z-1}P_{Z-1}(t) -(\Delta^{(+)}_Z+\Delta^{(-)}_Z+\Lambda^{qf}_Z)P_Z(t), \tag{4}$$

where $P_Z(0)=\delta_{ZZ_i}$ and the microscopically calculated transport coefficients $\Delta^{(\pm)}_Z$

$$\Delta^{(+)}_Z=\frac{1}{\Delta t}\sum_{P,T}|g_{PT}(R)|^2 n^Z_T(\Theta)[1-n^Z_P(\Theta)] \times\frac{\sin^2[\Delta t(\tilde{\epsilon}^Z_P-\tilde{\epsilon}^Z_T)/2\hbar]}{(\tilde{\epsilon}^Z_P-\tilde{\epsilon}^Z_T)^2/4},$$

$$\Delta^{(-)}_Z=\frac{1}{\Delta t}\sum_{P,T}|g_{PT}(R)|^2 n^Z_P(\Theta)[1-n^Z_T(\Theta)] \times\frac{\sin^2[\Delta t(\tilde{\epsilon}^Z_P-\tilde{\epsilon}^Z_T)/2\hbar]}{(\tilde{\epsilon}^Z_P-\tilde{\epsilon}^Z_T)^2/4} \tag{5}$$

characterize the probability rate of the proton transfer from a heavy to a light nucleus $(\Delta^{(+)}_Z)$ or in opposite direction $(\Delta^{(-)}_Z)$. The coefficient Λ^{qf}_Z is the rate of decay probability in R. The solution of master equations (4) with the decay terms and the microscopically calculated transport coefficients results in the realistic description of the DNS evolution in charge (mass) asymmetry. In our previous papers on fusion in the DNS model [5–9] Eq. (4) was not considered and the quasifission was treated in a simple manner. The use of Eq. (4) with Eq. (5) assumes an overdamped motion in Z and does not demand a separate calculation of the mass parameter in Z to describe the DNS dynamics. As shown in [5], the friction extracted from Eq. (4) is in agreement with other calculations.

In Eq. (4) we take only transitions $Z\rightleftharpoons Z+1$ and $Z\rightleftharpoons Z-1$ into account in the spirit of the independent-particle model. The indices "P" and "T" in Eqs. (5) are quantum numbers characterizing the single-particle states in the light and heavy nucleus, respectively, $n^Z_P(\Theta)$ $[n^Z_T(\Theta)]$ are the Fermi occupation numbers of the single-particle proton states in a light (heavy) nucleus depending on the temperature Θ, $g_{PT}=\langle P|0.5(U_P+U_T)|T\rangle$ are the matrix elements for the proton transition between nuclei by the action of the mean fields U_P and U_T of the DNS nuclei [14,18,26–32]. The time interval $\Delta t=1.5\times10^{-22}$ s is larger than the relaxation time of the mean field but considerably smaller than the characteristic evolution time of the macroscopic quantities. The mutual influence of the mean fields of the reaction partners leads to a renormalization of the single-particle energies $\epsilon_{P(T)}$ of noninteracting nuclei [14,18]. Due to the long-range character, the Coulomb interaction gives the main contribution to this renormalization. Thus, in Eq. (5) for protons approximately

$$\tilde{\epsilon}^Z_P-\tilde{\epsilon}^Z_T=\epsilon^Z_P-\epsilon^Z_T+(Z_T-Z_P)e^2/(2R),$$

where $Z_{P(T)}$ is the atomic number of a light (heavy) fragment. As was shown in [14] the Coulomb interaction increases the formation probability of very asymmetric configurations.

In order to simplify the calculation of the transport coefficients (5) for each Z, we used the single particle levels obtained with the spherical Woods-Saxon potentials, spin-orbit, and Coulomb interactions [14,18]. The examples of these level schemes are given in Ref. [27]. The energies of last occupied levels were normalized to describe the nucleon separation energies known from the experiment or self-consistent calculations [14,18]. As shown in [18,28], with this simplified procedure the peculiarities of the structure of the DNS nuclei are effectively taken into account in Eq. (5). Indeed, the values of $\Delta^{(\pm)}_Z$ depend on the sum over single particle states which is not crucial to the level splitting due to the deformation. The nucleon transfers mainly occur between the single-particle states near the Fermi levels of the DNS nuclei due to the action of the Pauli blocking factors $n^Z_{T(P)}(1-n^Z_{P(T)})$ and the selection rules in the matrix elements g_{PT}. In the calculations we do not fit any parameters, they are taken to be the same for all reactions considered.

In Ref. [26] the analytical method of the calculation of the matrix elements $g_{PT}(R)$ was suggested. This method (see Appendix) allows one to obtain the matrix elements for vari-

ous values of R. At $R \geqslant R_{\epsilon_P} + R_{\epsilon_T}$ [$R_{\epsilon_{P(T)}}$ is the radius of sewing for internal and external parts of the wave function of the state $P(T)$] we have

$$g_{PT}(R) = (-1)^{l_T + m_T + 1/2} C^{\rm ex}_{l_T} C^{\rm ex}_{l_P} \sqrt{(2j_P+1)(2j_T+1)} \times \sum_L \left(j_T - \frac{1}{2}, j_P \frac{1}{2} \middle| L0 \right) (j_T - m_T, j_P m_P | L0) \times [A_P k_L(\varpi_P R) + A_T k_L(\varpi_T R)]. \quad (6)$$

At $R < R_{\epsilon_P} + R_{\epsilon_T}$ the following expression has to be used:

$$g_{PT}(R) = (-1)^{l_T + m_T + 1/2} C^{\rm ex}_{l_T} C^{\rm ex}_{l_P} \sqrt{(2j_P+1)(2j_T+1)} \times \sum_L \left(j_T - \frac{1}{2}, j_P \frac{1}{2} \middle| L0 \right) (j_T - m_T, j_P m_P | L0) \times \{(-1)^{(L - l_T - l_P)/2} [B_P y_L(\kappa_P R) + B_T y_L(\kappa_T R) + D_P j_L(\kappa_P R) + D_T j_L(\kappa_T R)] + G_P k_L(\varpi_P R) + G_T k_L(\varpi_T R) + I^0_{PT}(R,L)\}. \quad (7)$$

Here, $j_L(x)$, $k_L(x)$, $y_L(x)$ are the spherical Bessel functions [29], $l_{P(T)}$ and $j_{P(T)}$ are the orbital and total single particle momenta, respectively, $m_{P(T)}$ is the projection of $j_{P(T)}$. The dependences of normalized coefficient $C^{\rm ex}_{l_{P(T)}}$, constants $A_{P(T)}$, $B_{P(T)}$, $D_{P(T)}$, $G_{P(T)}$, and value of $I^0_{PT}(R,L)$ on single particle quantum numbers are given in Appendix. The wave numbers for external and internal parts of the wave function are determined by the relations

$$\varpi_{P(T)} = \sqrt{\frac{2m}{\hbar^2}[B_{Coul} - \epsilon_{P(T)}]},$$

$$\kappa_{P(T)} = \sqrt{\frac{2m}{\hbar^2}[\epsilon_{P(T)} - \overline{U}_{P(T)}]},$$

where $\overline{U}_{P(T)} = \langle P(T) | U_{P(T)} | P(T) \rangle$ is the average value of the single particle potential of light (heavy) nuclei over state $P(T)$, m is the proton mass, B_{Coul} is the Coulomb barrier of the nucleus for protons.

B. Decay rate of the DNS

The DNS potential energy is required for calculating the decay rates Λ^{qf}_Z in Eq. (4). This potential can be derived from the microscopically calculated transport coefficients (5) [18,28]. However, since the study of the DNS evolution with a microscopically obtained potential is similar [14] to the one with the phenomenologically calculated potential [5,28], we use for simplicity the latter one in the following. It is given as

$$U(R,Z,J) = B_1 + B_2 + V(R,Z,J) - [B_{12} + V'_{rot}(J)], \quad (8)$$

where B_1, B_2, and B_{12} are the binding energies of the fragments and the compound nucleus, respectively. The value of $U(R,Z,J)$ is normalized to the energy of the rotating compound nucleus by $B_{12} + V'_{rot}$. The nucleus-nucleus potential [5,28]

$$V(R,Z,J) = V_C(R,Z) + V_N(R,Z) + V_{rot}(R,Z,J) \quad (9)$$

in Eq. (8) is the sum of the Coulomb potential V_C, the nuclear potential $V_N(R,Z)$, and the centrifugal potential $V_{rot}(R,Z,J)$. For the nuclear part of $V(R,Z,J)$ we use a double folding formalism with the effective density-dependent nucleon-nucleon interaction [5] which is known from the theory of finite Fermi systems. As a result of numerous calculations, the simple approximate expression can be suggested for $V_N(R,Z)$

$$V_N(R,Z) = V_0[\exp(-2(R - R_{PT})\alpha/R_{PT}) - 2\exp(-(R - R_{PT})\alpha/R_{PT})],$$

$$V_0 = 2\pi a_P a_T \overline{R}(11.3 - 0.82\overline{R}),$$

$$\alpha = 11.47 - 17.32 a_P a_T + 2.07\overline{R}, \quad (10)$$

$$\overline{R} = R_P R_T / R_{PT}, \quad R_{PT} = R_P + R_T, \quad R_{P(T)} = r_0 A^{1/3}_{P(T)},$$

where $r_0 = 1.14$–1.16 fm, the diffuseness $a_{P(T)} = 0.52$–0.55 fm, and $R_{P(T)}$ is the radius of nucleus ''P''(''T'') . The influence of the rotational energy on Eq. (8) is negligible [5] for heavy systems considered here and small values of the angular momentum. Deformation effects are taken into account in the calculation of $V(R,Z,J)$. Deformed nuclei are treated in the pole-to-pole orientation. For ground state deformations of the nuclei, the deformations mainly influence $V(R,Z,J)$ through V_C.

For $R_P + R_T - 1$ fm $< R < R_P + R_T + 2$ fm, the potential $V(R,Z,J)$ has a pocket as a function of the relative distance R with a small depth which results from the attractive nuclear and repulsive Coulomb interactions. As follows numerous calculations of the nucleus-nucleus potential with nuclear part in the double-folding form [5], the bottom of the pocket is situated at the distance $R_m = R_P + R_T + 0.5$ fm. The decaying DNS has to overcome the potential barrier B_{qf} [5] which value coincides with the depth of this pocket. The values of B_{qf}, depending on Z, mainly determine the lifetime t_0 of the DNS. Since we consider reactions with heavy nuclei which occur slightly above the Coulomb barrier at $R \approx R_P + R_T + 2$ fm, partial waves with angular momenta less than $30\hbar$ contribute to the yield of quasifission products with Z far from Z_i, and the values of the quasifission barrier B_{qf} weakly depend on angular momentum J because of the large moment of inertia of the DNS.

The decay of the DNS in R can be treated with the one-dimensional Kramers rate [33–35] Λ^{qf}_Z of probability

$$\Lambda^{qf}_Z = \frac{\omega}{2\pi\omega^{B_{qf}}} \left(\sqrt{\left(\frac{\Gamma}{2\hbar}\right)^2 + (\omega^{B_{qf}})^2} - \frac{\Gamma}{2\hbar} \right) \exp\left(- \frac{B_{qf}(Z)}{\Theta} \right), \quad (11)$$

which exponentially depends on the quasifission barrier $B_{qf}(Z)$ for a given charge (mass) asymmetry Z [5]. The height B_{qf} of this barrier uniformly decreases with increasing Z because the increasing Coulomb repulsion leads to very shallow pockets in the nucleus-nucleus potential for near symmetric configurations. The temperature $\Theta(Z)$ is calculated by using the Fermi-gas expression $\Theta=\sqrt{E^*/a}$ with the excitation energy $E^*(Z)$ of the DNS and with the level-density parameter $a=A_{tot}/12$ MeV^{-1}, where A_{tot} is the total mass number of the system. If the fusion barrier in Z coordinate is located at $Z=Z_{BG}$, the excitation energy $E^*(Z)$ of the DNS increases with decreasing Z for $Z<Z_{BG}$ and increasing Z for $Z>Z_{BG}$. The calculated DNS potential energy surfaces as function of Z have fusion barriers at $Z_{BG}=7-9$ in the cold and hot fusion reactions considered. In Eq. (11), $\omega^{B_{qf}}$ is the frequency of the inverted harmonic oscillator approximating the potential V in R around the top of the quasifission barrier at $Z=Z_{BG}$, and ω is the frequency of the harmonic oscillator approximating the potential in R at the bottom of the pocket. The local oscillator approximation of the potential energy surface is good, and we can neglect the nondiagonal components of the curvature tensor. The method of the calculation of the mass parameters needed to obtain the frequencies is given in [36]. The mass of the DNS in the R coordinate is close to the reduced mass and the nondiagonal mass coefficient for R and Z motions is small. Therefore, the one-dimensional Kramers rate (11) gives similar results as the quasifission rates over a two-dimensional potential barrier in the space (R,Z) [5]. The constant values $\hbar\omega^{B_{qf}}=1.0$ MeV and $\hbar\omega=2.0$ MeV are used for the reactions considered in the following. Further, we set $\Gamma=2$ MeV in Eq. (11) which means that the friction coefficient in R has the same order of magnitude as the one calculated within one-body dissipation models [15,5]. The possibility to apply the Kramers expression to relatively small barriers was demonstrated in [37]. Since the transient times are quite short for the considered excitations energies E^* and quasifission barriers B_{qf}, the use of the expressions (12) and (11) are justified. As in fission where other channels are involved as well, the Kramers formula is suitable in our case within the accuracy of the calculation of the potential barriers.

C. Charge (mass) yield for quasifission

The measurable charge (mass) yield for quasifission can be expressed by the product of the formation probability $P_Z(t)$ of the DNS configuration with charge (mass) asymmetry Z and the decay probability in R represented by the quasifission rate Λ_Z^{qf}:

$$Y_Z(t_0)=\Lambda_Z^{qf}\int_0^{t_0}P_Z(t)dt. \tag{12}$$

Here, t_0 is the time of reaction which is determined by solving the equation

$$\sum_Z \Lambda_Z^{qf}\int_0^{t_0}P_Z(t)dt=1-P_{CN},$$

where $P_{CN}=\Sigma_{Z<Z_{BG}}P_Z(t_0)$, i.e., the fusion probability is defined by the fraction of probability existing at time t_0 for $Z<Z_{BG}$. With this definition the calculated values of P_{CN} practically coincide with those obtained in [7] with the other method. Mainly the decay of the DNS with $Z>Z_{BG}$ contributes to the quasifission yield. The DNS with $Z<Z_{BG}$ are assumed to evolve to the compound nucleus with a high probability. The characteristic time (a few units of 10^{-21} s) of this evolution is shorter than the decay time of unstable (the lifetime is shorter than the shortest time for the experimental detection) superheavy compound nucleus or unstable superheavy nucleus in the very asymmetric DNS. Because of this we separate two processes: the formation and the survival of superheavy nucleus.

A yield of the quasifission products with very small Z could be seen only in reactions with a quite large mass (charge) asymmetry in the entrance channel. For large angular momenta and excitation energies which are not considered here, a decay of the DNS with $2<Z<Z_{BG}$ becomes more pronounced [30]. The factors $P_Z(t)$ and Λ_Z^{qf} in Eq. (12) are considered separately because the characteristic time for nucleon transitions between the nuclei is much shorter than the decay time of the DNS. Earlier calculations [14,18,31,32] of charge (mass) distributions in deep-inelastic collisions, which occur during much shorter time than the quasifission, were performed without the decay rate Λ_Z^{qf} in Eq. (4) but assuming simply $Y_{Z(A)}(t_0)\approx P_{Z(A)}(t_0)$ with t_0 as a free parameter. With the decay rate in Eq. (4) the description of the DNS evolution becomes self-consistent. The yield $Y_{Z(A)}$ calculated without decay term in Eq. (4) at quite large time $t=t_0$ can deviate from the experimental data. Therefore, the incorporation of the decay term in Eq. (4) is very important for the description of the DNS evolution for quite a long time.

III. RESULTS AND DISCUSSION

A. Important elements of computations

In the calculations with Eq. (4) the isotopic composition of the nuclei forming the DNS is chosen from the condition of a N/Z equilibrium in the system. As follows from the experimental data on deep inelastic collisions [15] and our previous calculations [14], the N/Z equilibrium in the DNS is mainly established by the nucleon exchange in quite a short time after the DNS formation. Therefore, in our calculations of the quasifission, which is a slower process than a deep inelastic collision, collective contributions (like a large amplitude dipole mode) can be neglected.

The transport coefficients $\Delta_Z^{(\pm)}$ in Eq. (4) are calculated as described in Sec. II A with realistic single particle level schemes. Due to the Pauli blocking factors $n_{T(P)}^Z(1-n_{P(T)}^Z)$ in Eq. (5) and the selection rules in the matrix elements g_{PT}, only about ten levels near the Fermi level of each nucleus are necessary to determine $\Delta_Z^{(\pm)}$. The results of the present paper could be slightly improved in more complicated calculations without reasonable simplification made in Sec. II A for incorporating the level schemes in Eq. (5).

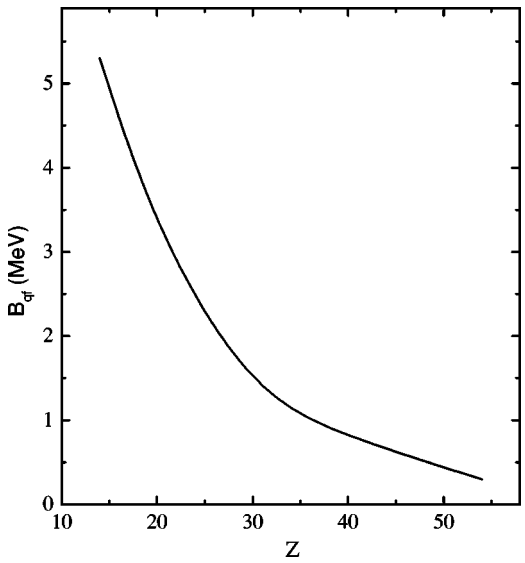

FIG. 1. Calculated dependence of the quasifission barrier B_{qf} on Z in the DNS formed in the ^{48}Ca+^{238}U reaction at $J=0$.

The quasifission distributions of charge and mass slightly depend on the excitation energy E^* of the initial DNS (Fig. 2). This is due to a weak dependence of the transport coefficients $\Delta_Z^{(\pm)}$ on the temperature [14]. With an increasing temperature of the system, the influence of the shell effects on the process of nucleon transfer decreases more slowly than the exponential decrease of the shell correction to the potential energy. Although the nucleon exchange increases with the temperature, this effect is rather weak in the considered interval of excitation energy. The factors suppressing the growth of the neck and melting of the DNS in R survive at even higher temperature [25]. It was experimentally found [11] in the quasifission reactions ^{238}U+^{16}O, ^{26}Mg, ^{27}Al, ^{32}S, ^{35}Cl, ^{40,48}Ca, and $^{\text{nat}}$Zn at several bombarding energies, that the motion in mass asymmetry is dominated by the one-body dissipation which is independent of temperature. Since one can describe [14] many experimental data of deep inelastic collisions with a one-body dissipation, one can assume that the inclusion of a two-body dissipation creates minor changes in the results which are within the accuracy of the definition of the parameters used.

If in the vicinity of some $Z\Delta_Z^{(+)}$ is close to $\Delta_Z^{(-)}$ and the inequalities $\Delta_Z^{(+)}>\Delta_Z^{(-)}$ and $\Delta_Z^{(+)}<\Delta_Z^{(-)}$ hold for smaller and larger Z, respectively, or $\Delta_Z^{(+)}$ and $\Delta_Z^{(-)}$ are minimal with respect to those for neighboring Z, the distribution P_Z has local maximum at this Z [38]. For example, in the ^{48}Ca $+^{238}$U reaction this occurs at $Z=30$–32, 42–44, 54, and 56. While the difference between the Fermi levels of heavy and light nuclei is 8.2 MeV in the system ^{74}Ni+^{212}Po, it is 2 MeV in the system ^{80}Ge+^{206}Hg. As a result, $\Delta_Z^{(+)}$ ($\Delta_Z^{(-)}$) decreases (increases) when the DNS passes the configuration with ^{208}Pb. If in the entrance DNS $\Delta_Z^{(+)}\approx\Delta_Z^{(-)}$, then the charge (mass) distribution has maximum at $Z=Z_i$. One can expect this in the reactions with lead. The maxima and minima of P_Z as a function of Z correlate with minima and maxima in the DNS potential energy as a function of Z at $R=R_m(Z)$, respectively [28].

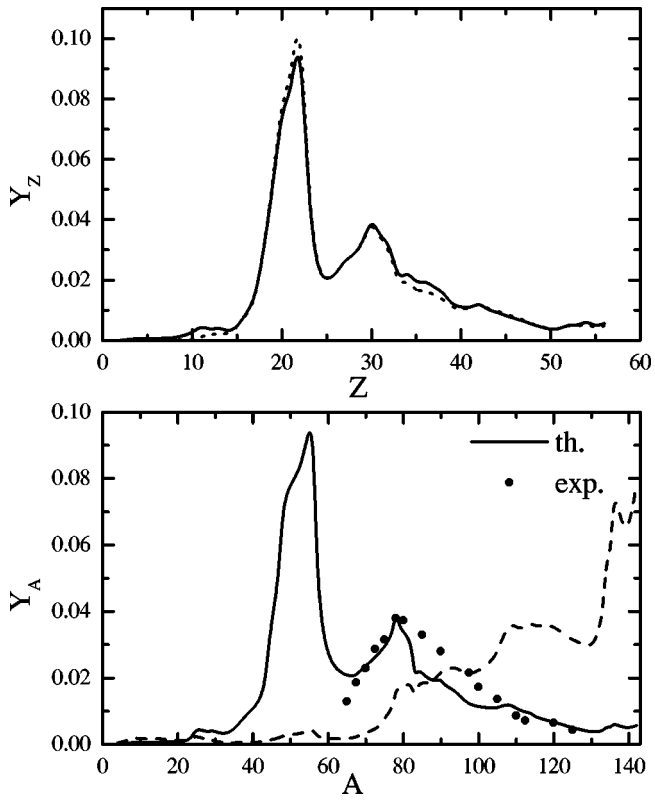

FIG. 2. Charge (upper part) and mass (lower part) yields, Y_Z and Y_A, of the quasifission products as a function of the charge (Z) and mass (A) numbers of the light fragments, respectively, for the hot fusion reaction ^{48}Ca+^{238}U$\rightarrow^{286}$112. The charge distribution is calculated for two values of the excitation energy of the initial DNS: $E^*=5$ MeV (dotted line) and $E^*=10$ MeV (solid line). The mass distribution is compared with experimental data [12] (solid points) for $E^*=10$ MeV (the initial DNS) which corresponds to the excitation energy of compound nucleus of about 33 MeV. For $E^*=10$ MeV, the distribution of the DNS in A calculated with Eq. (4) and $\Lambda_Z^{qf}=0$ at $t=t_0=3.5\times10^{-20}$ s is presented by the dashed line (lower part).

The decay rate of the DNS is calculated using the value of B_{qf} determined with the potential (9). The dependence of B_{qf} on Z in the DNS formed in the ^{48}Ca+^{238}U reaction is shown in Fig. 1. Although the values of fusion barrier B_{fus}^* are not directly used in the present calculations, we show them to demonstrate its correlation with the fusion probability.

In all reactions considered here the lifetime t_0 of the DNS is about $(3-4)\times10^{-20}$ s that is in agreement with time extracted from experimental data [39]. In Fig. 2 the distribution of the DNS in mass asymmetry is presented at $t=t_0=3.5\times10^{-20}$ s for the case of $\Lambda_Z^{qf}=0$ in Eq. (4). The maximum of this distribution is expected to correspond to the minimum of the potential energy as a function of Z at symmetric DNS, $Z\approx Z_{tot}/2$ [28]. Since B_{qf} decreases with increasing Z (Fig. 1), the decay of the DNS, when it moves in Z, prohibits the formation of configurations with large Z. The calculation with $\Lambda_Z^{qf}\neq0$ in Eq. (4) leads to much smaller yield of symmetric DNS. Thus, the account of the decay term is very important for correct description of the yield of

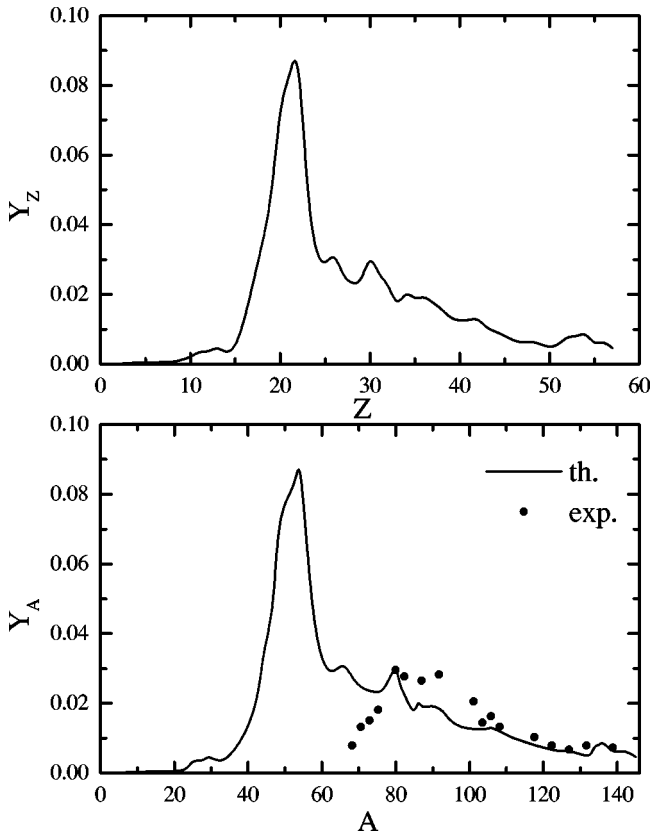

FIG. 3. The same as in Fig. 2, but for the hot fusion reaction ^{48}Ca+^{244}Pu→^{292}114. The experimental mass distribution (solid points) is taken from Ref. [12]. The excitation energy of the initial DNS is $E^*=10$ MeV.

quasifission products which are formed during time t_0 at least 10 times larger than the characteristic time of deep inelastic collisions.

The decrease of quasifission cross section $\sigma_{qf}(E_{\text{c.m.}},A)=\sigma_{cap}(E_{\text{c.m.}})Y_A(t_0)$ and increase of asymmetry of mass distribution with decreasing bombarding energy (excitation energy of the initial DNS) under the Coulomb barrier [12] can be mainly explained by the reduction of $\sigma_{cap}(E_{\text{c.m.}})$. In our calculations we assume that the DNS is formed in all reactions considered.

B. Hot fusion reactions

Figures 2 and 3 show the calculated charge and mass distributions of quasifission products for hot fusion reactions with the projectile ^{48}Ca on the targets ^{238}U and ^{244}Pu [2,11,12], which lead to the synthesis of the elements ^{286}112 and ^{292}114, respectively. Only the part of the quasifission charge (mass) distributions corresponding to the light fragments is depicted. The distributions reveal large widths, and one can observe a notable drift in mass and charge away from the initial mass (charge) asymmetry. The masses of products are substantially different from the initial target-projectile masses and symmetric fragments can be formed with a quite large cross section. The main peak of the charge and mass distributions is around the initial configuration of the DNS. Since the calculations were performed with angular momenta less than the critical angular momentum and deep-inelastic or quasielastic collisions were not considered, the main calculated peak corresponds to quasifission. The quasifission barriers are rather small in the entrance channel of the reactions considered. If the quasifission barrier for the initial mass asymmetry would be larger, this peak would not be so pronounced and even could vanish. The figures show no experimental points in this mass region because of the difficulties to discriminate the quasifission events from the products of deep inelastic or quasielastic collisions.

The calculated charge (mass) distributions of quasifission products are in good agreement with the available experimental data [12] (Figs. 2 and 3). The structures in the distribution of quasifission products reflect the influence of the shell effects in the DNS nuclei on the nucleon-exchange process, especially the maxima in the charge (mass) distributions are related to the decay of the DNS consisting of magic or semimagic nuclei. The absence of local peaks for some magic nuclei is explained by the shell structure of the conjugated nucleus and the influence of the neutron subsystem. In the reactions ^{48}Ca+^{238}U [$P_{CN}\approx10^{-2}$, $B^*_{fus}=8.5$ MeV, $B_{qf}(Z_i=20)=3.2$ MeV], and ^{48}Ca+^{244}Pu [$P_{CN}\approx10^{-3}$, $B^*_{fus}=10.5$ MeV, $B_{qf}(Z_i=20)=3.1$ MeV] the maximum yield of the quasifission fragments occurs around the nucleus ^{208}Pb for the heavy fragment where the DNS potential energy has a minimum [28]. Together with the decay term in Eq. (4) this suppresses the evolution of the DNS to smaller mass asymmetry and, correspondingly, increases the decay probability from such configuration. In reaction ^{48}Ca $+^{238}$U (^{48}Ca+^{244}Pu) the height of this peak is 6 (3) times larger the height of peaks in the symmetric mass region.

The experimental fusion probability P_{CN} becomes smaller with decreasing mass asymmetry in the entrance channel [40]. The fusion cross section depends also on the nuclear shells but not so strongly as the decay process of the compound nucleus. For example, the dependence of experimental fusion probability on the $Z_1\times Z_2$ in the entrance channel shows the strong macroscopic trend which is related to the change of the Coulomb interaction between nuclei and to the small fluctuations around this trend due to shell structure of fusing nuclei [40,41,7]. The value of excitation energy E^*_{CN} of the formed compound nucleus is related to the bombarding energy $E_{\text{c.m.}}=E^*_{CN}-Q$ which exceeds the Coulomb barrier by the value $E^*_{CN}-[U(R_m,Z=20)+B_{qf}(Z=20)]=E^*-B_{qf}(Z=20)$. In actinides based reactions the value of $E^*=10$ MeV was taken in the calculations to supply $E^*_{CN}\approx35$ MeV.

Taking the deformation of the nuclei in the DNS [5] in the ^{48}Ca+^{238}U reaction into account, we find that the calculated average total kinetic energy $\langle TKE\rangle=240$ MeV of the quasifission products with $70<A<120$ is in agreement with the experimental data [11] and the systematics [42]. Considering the fluctuations of the DNS charge asymmetry (the fluctuations of the Coulomb interaction) at fixed mass asymmetry, the fluctuations of the quadrupole deformation parameters of the DNS nuclei and the fluctuations of the bending mode in the DNS, it is possible to explain the large variance of the TKE distribution as a function of the mass numbers of the

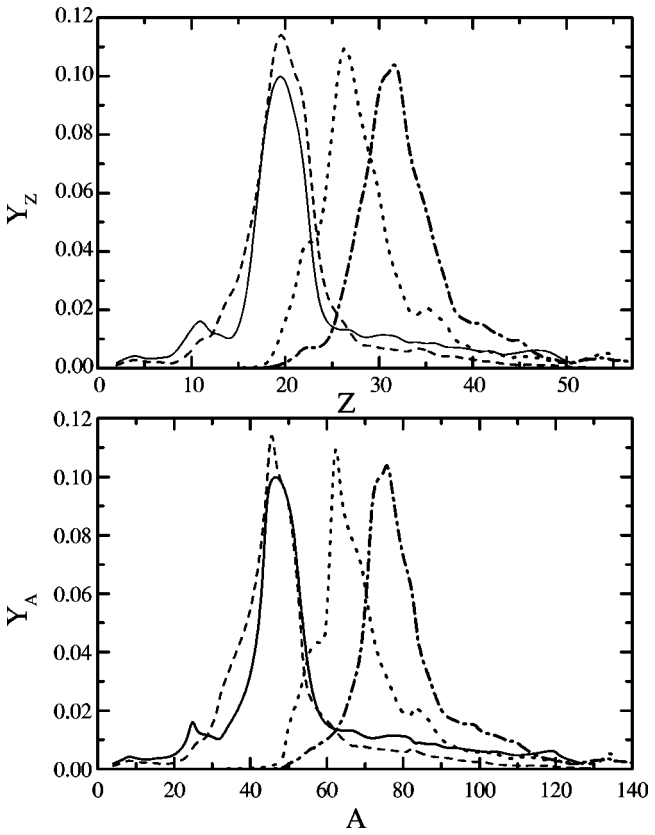

FIG. 4. Charge (upper part) and mass (lower part) yields, Y_Z and Y_A, of the quasifission products as a function of the charge (Z) and mass (A) numbers of the light fragments, respectively, for the cold fusion reactions ^{48}Ca+^{208}Pb$\rightarrow^{256}$102 (solid curves), ^{50}Ti+^{208}Pb $\rightarrow^{258}$104 (dashed curves), ^{64}Ni+^{208}Pb$\rightarrow^{272}$110 (dotted curves), and ^{76}Ge+^{208}Pb$\rightarrow^{284}$114 (dashed-dotted curves). The charge and mass distributions are calculated for the excitation energy $E^*=10$ MeV of the initial DNS.

fragments. Investigations in this direction are in progress.

C. Cold fusion reactions

The calculations of quasifission products for the cold fusion reactions are important for the planned quasifission experiments in many laboratories. Figure 4 shows the quasifission distributions of charge and mass for the cold fusion reactions with the projectiles ^{48}Ca [$P_{CN}\approx 5\times10^{-1}$, $B^*_{fus}=5.5$ MeV, $B_{qf}(Z_i=20)=5.3$ MeV], ^{50}Ti [$P_{CN}\approx 3\times10^{-2}$, $B^*_{fus}=4.7$ MeV, $B_{qf}(Z_i=22)=4.0$ MeV], ^{64}Ni [$P_{CN}\approx 10^{-5}$ $B^*_{fus}=7.2$ MeV, $B_{qf}(Z_i=28)=1.4$ MeV], and ^{76}Ge [$P_{CN}\approx 4\times10^{-9}$, $B^*_{fus}=14.7$ MeV, $B_{qf}(Z_i=32)=0.6$ MeV] on the target ^{208}Pb, which lead to the synthesis of the elements ^{256}102, ^{258}104, ^{272}110, and ^{284}114, respectively, with an excitation energy of about (11–16) MeV [1]. The ratio between the motions of the DNS to more symmetric and more asymmetric configurations increases exponentially with an increasing charge number of the superheavy compound nucleus. Due to this fact, complete fusion in the DNS model related to the diffusion of the system to more asymmetric configurations decreases by several orders of magnitude from the compound nucleus ^{258}104 to ^{278}112 [1]. It is seen that in the Pb-based reactions the charge and mass distributions have no pronounced maxima besides the main peak around the entrance DNS (Fig. 4). This structure of the mass (charge) distribution of the quasifission products well corresponds to the peculiarities of the DNS potential energy which has the consequence that the DNS consisting of such strongly bound nuclei like ^{208}Pb for $Z>Z_i$ are absent.

The form of the mass and charge distributions change much from the reaction ^{48}Ca+^{208}Pb$\rightarrow^{256}$No (Fig. 4) to the reactions ^{48}Ca+^{238}U, ^{244}Pu$\rightarrow^{286}$112,^{292}114 (Figs. 2 and 3). In the reactions leading to the nuclei ^{286}112 and ^{292}114 the decay of the more symmetric DNS configurations is more pronounced. The motion of the initial DNS to more asymmetric configurations (mass asymmetry channel of fusion) is more favored in the reaction ^{48}Ca+^{208}Pb than in the reactions ^{48}Ca+^{238}U and ^{48}Ca+^{244}Pu where the distributions show similar features for $Z<20$ and $A<48$. This has as a consequence that the fusion probability in the mass asymmetry coordinate is significantly larger in the ^{48}Ca+^{208}Pb reaction.

Comparing Fig. 4 with Fig. 3, we see that the mass and charge yields of the quasifission products for near symmetric configurations of the DNS are larger for the hot fusion reaction ^{48}Ca+^{244}Pu than for the cold fusion reaction ^{76}Ge +^{208}Pb. In the cold and hot fusion reactions considered for the synthesis of the 114 elements, the excitation energies of the initial DNS are practically the same and the excitation energies of the compound nuclei are different mainly due to the difference between the Q values. Since the quasifission barrier B_{qf} increases with decreasing Z and increasing neutron number of the system, the difference between the quasifission distributions in cold and hot fusion reactions is related to different choices of the colliding nuclei. We found for the reaction ^{76}Ge+^{208}Pb$\rightarrow^{284}$114, that the quasifission products are practically associated with fragmentations near the initial DNS due to the small values of the quasifission barriers B_{qf}. This is consistent with the conclusion that the hot fusion reaction ^{48}Ca+^{244}Pu$\rightarrow^{292}$114 is preferable for the synthesis of the element 114, although the survival probability of the compound nucleus decreases with increasing excitation energy [6,9]. Indeed, the synthesis of the nucleus with $Z=114$ was reported in the reactions ^{48}Ca+^{242,244}Pu $\rightarrow^{287,289}$114+3n [2] and ^{48}Ca+^{244}Pu$\rightarrow^{288}$114+4n [3] with a cross section of about 1 pb. Our calculations [6] within the dinuclear system model give approximately the same value as in experiment.

IV. SUMMARY

The main conclusions are (1) The diffusion in charge (mass) asymmetry and in relative distance (the DNS decay) coordinates contributes to the yields of quasifission products. The calculated characteristic quasifission time is about $(3-4)\times10^{-20}$ s which is in agreement with time extracted from experimental data. (2) The quasifission products of hot fusion reactions ^{48}Ca+^{244}Pu and ^{48}Ca+^{238}U are correctly described with the DNS model. The estimated average total kinetic energy of the quasifission products is in agreement

with the experimental data and the empirical systematics. (3) For the cold fusion reactions leading to the superheavy elements the quasifission products are practically associated with fragmentations near the initial (entrance) DNS. Such examples are the reactions ^{64}Ni+^{208}Pb, ^{70}Zn +^{208}Pb, ^{76}Ge+^{208}Pb, etc. (4) If the compound nucleus is quite stable to be detected, the quasifission process is the main factor suppressing the complete fusion of heavy nuclei. In fusion reactions the fusion-fission events are much smaller than the events of the production of certain quasifission products. The main contribution to symmetric and near symmetric fragmentations comes from quasifission process. (5) Since the quasifission dominates in the cold and hot fusion reactions, a comparison of theoretical and experimental data of quasifission constitutes a critical test for the dynamics of existing fusion models.

ACKNOWLEDGMENTS

We thank Professor R.V. Jolos, Professor V.V. Volkov, Dr. E.A. Cherepanov, Dr. A.B. Larionov, and Dr. A.K. Nasirov for fruitful discussions and suggestions. G.G.A. and A.D.-T. are grateful for the support of the Alexander von Humboldt-Stiftung and DAAD, respectively. This work was supported in part by DFG and RFBR, STCU, SCST of RV$_Z$, VFBR.

APPENDIX A

In order to calculate the matrix element

$$g_{PT}(R)=\frac{1}{2}\int d\mathbf{r}\psi_T^*(\mathbf{r})[U_T(\mathbf{r})+U_P(\mathbf{r}-\mathbf{R})]\psi_P(\mathbf{r}-\mathbf{R}),$$

we approximate the radial parts of wave functions by the wave functions of rectangle box with the depth $\overline{U_i}$ $(i=P,T)$, where $\overline{U}_{P(T)}$ is the average value of the single particle potential of light (heavy) nuclei over the state $P(T)$,

$$\psi_i(\mathbf{r})=\psi_{l_i}(r)\sum_{m\sigma}(l_i m,1/2\sigma|j_i m_i)Y_{l_i m_i}(\theta,\phi)\chi_\sigma,$$

$$\psi_{l_i}(r)=\begin{cases} C_{l_i}^{\rm in} j_{l_i}(\kappa_i r), & r\leqslant R_{\epsilon_i},\\ C_{l_i}^{\rm ex} k_{l_i}(\varpi_i r), & r\geqslant R_{\epsilon_i}.\end{cases}$$

For each state with energy ϵ_i, the value of R_{ϵ_i} is defined from $U_i(R_{\epsilon_i})=\epsilon_i$. The spherically symmetric potentials are treated here. Taking into account the continuities of the wave function at R_{ϵ_i} and normalization condition, we obtain

$$C_{l_{P(T)}}^{\rm ex}=\sqrt{2}\Bigg[R_{\epsilon_{P(T)}}^3\left(1+\frac{\varpi_{P(T)}^2}{\kappa_{P(T)}^2}\right)k_{l_{P(T)}+1}(\varpi_{P(T)}R_{\epsilon_{P(T)}})\times k_{l_{P(T)}-1}(\varpi_{P(T)}R_{\epsilon_{P(T)}})\Bigg]^{-1/2},$$

$$C_{l_{P(T)}}^{\rm in}=\frac{k_{l_{P(T)}}(\varpi_{P(T)}R_{\epsilon_{P(T)}})}{j_{l_{P(T)}}(\kappa_{P(T)}R_{\epsilon_{P(T)}})}C_{l_{P(T)}}^{\rm ex}.$$

Using the Fourier transformations of the wave functions, one can obtain

$$\begin{aligned} g_{PT}(R)&=\frac{1}{2}\int d\mathbf{p}e^{i\mathbf{pR}}\psi_T^*(\mathbf{p})\left[\left\{\epsilon_T-\frac{\hbar^2}{2m}p^2\right\}+\left\{\epsilon_P-\frac{\hbar^2}{2m}p^2\right\}\right]\psi_P(\mathbf{p})\\ &=\frac{(-1)^{m_T-1/2}}{2}\sqrt{(2j_P+1)(2j_T+1)}\\ &\quad\times\sum_L i^L(j_T-1/2,j_P1/2|L0)(j_T-m_T,j_Pm_P|L0)\\ &\quad\times\int_0^\infty dpp^2j_L(pR)\left[\left\{\epsilon_T-\frac{\hbar^2}{2m}p^2\right\}+\left\{\epsilon_P-\frac{\hbar^2}{2m}p^2\right\}\right]\psi_{l_T}^*(p)\psi_{l_P}(p).\end{aligned}$$

The integrand in this expression has poles at $p=\pm i\varpi_{P(T)}$, $\pm\kappa_{P(T)}$. Calculating the residues, we obtain Eq. (6) for $R>R_{\epsilon_P}+R_{\epsilon_T}$, where

$$A_{P(T)}=d_{P(T)}\xi[i_{l_{T(P)}}(\varpi_{P(T)}R_{\epsilon_{T(P)}})]$$

and

$$d_{P(T)}=\frac{(\epsilon_P+\epsilon_T+\hbar^2\varpi_{P(T)}^2/m)(\varpi_{T(P)}^2+\kappa_{T(P)}^2)R_{\epsilon_{P(T)}}^2}{2(\varpi_{P(T)}^2+\kappa_{T(P)}^2)(\varpi_{P(T)}^2-\varpi_{T(P)}^2)}$$

$$\xi[f_{l_{P(T)}}(\kappa' R_{\epsilon_{P(T)}})]=f_{l_{P(T)}}^2(\kappa' R_{\epsilon_P(T)})\frac{\partial}{\partial R_{\epsilon_{P(T)}}}\left(\frac{k_{l_{P(T)}}(\varpi_{P(T)}R_{\epsilon_{P(T)}})}{f_{l_{P(T)}}(\kappa' R_{\epsilon_{P(T)}})}\right).$$

Here, $f_{l_{P(T)}}(x)$ is one of the spherical Bessel functions.

In Eq. (7) obtained for $R\leqslant R_{\epsilon_P}+R_{\epsilon_T}$ the constants $B_{P(T)}$, $D_{P(T)}$, and $G_{P(T)}$ are

$$\begin{aligned} B_{P(T)}&=b_{P(T)}[\xi(y_{l_{T(P)}}(\kappa_{P(T)}R_{\epsilon_{T(P)}}))\xi(y_{l_{P(T)}}(\kappa_{P(T)}R_{\epsilon_{P(T)}}))\\ &\quad-\xi(j_{l_{T(P)}}(\kappa_{P(T)}R_{\epsilon_{T(P)}}))\xi(j_{l_{P(T)}}(\kappa_{P(T)}R_{\epsilon_{P(T)}}))],\\ D_{P(T)}&=b_{P(T)}[\xi(j_{l_{T(P)}}(\kappa_{P(T)}R_{\epsilon_{T(P)}}))\xi(y_{l_{P(T)}}(\kappa_{P(T)}R_{\epsilon_{P(T)}}))\\ &\quad+\xi(y_{l_{T(P)}}(\kappa_{P(T)}R_{\epsilon_{T(P)}}))\xi(j_{l_{P(T)}}(\kappa_{P(T)}R_{\epsilon_{P(T)}}))],\\ G_{P(T)}&=\frac{(-1)^{l_{P(T)}}}{\pi}d_{P(T)}\xi(k_{l_{T(P)}}(\varpi_{P(T)}R_{\epsilon_{T(P)}})),\end{aligned}$$

where

$$b_{P(T)}=\frac{\kappa_{P(T)}(\epsilon_P+\epsilon_T-\hbar^2\kappa_{P(T)}^2/m)(\kappa_{T(P)}^2+\varpi_{T(P)}^2)R_{\epsilon_P}^2R_{\epsilon_T}^2}{4(\kappa_{P(T)}^2+\varpi_{T(P)}^2)(\kappa_{T(P)}^2-\kappa_{P(T)}^2)}.$$

If $\varpi_P=\varpi_T$ or $\kappa_P=\kappa_T$ the corresponding limit of Eq. (6) or Eq. (7) is calculated. Since in Eq. (7) the term $I^0_{PT}(R,L)$ arising from the pole of the integrand at $p=0$ weakly depends on R and its analytical expression is very complicated, we replaced this term by its value at $R=R_{\epsilon_P}+R_{\epsilon_T}$ which is calculated from the comparison Eqs. (6) and (7).

[1] S. Hofmann and G. Münzenberg, Rev. Mod. Phys. **72**, 733 (2000).

[2] Yu. Ts. Oganessian *et al.*, Eur. Phys. J. A **5**, 63 (1999); Phys. Rev. Lett. **83**, 3154 (1999); A. V. Yeremin, V. K. Utyonkov, and Yu. Ts. Oganessian, in *Tours Symposium on Nuclear Physics III*, edited by M. Arnould, M. Lewitowicz, Yu. Ts. Oganessian, M. Ohta, H. Utsunomiya, and T. Wada, AIP Conf. Proc. No. 425 (AIP, Woodbury, 1998), p. 16.

[3] Yu. Ts. Oganessian *et al.*, Phys. Rev. C **62**, 041604(R) (2000).

[4] V. V. Volkov, in *Proceedings of the International School-Seminar on Heavy Ion Physics*, D7-87-68 (JINR, Dubna, 1987), p. 528; Izv. Akad. Nauk SSSR, Ser. Fiz. **50**, 1879 (1986); in *Proceedings of the 6th International Conference on Nuclear Reaction Mechanisms*, edited by E. Gadioli (Ricerca Scientifica ed Educazione Permanente Supplemento n. 84, Milan, 1991), p.39.

[5] N. V. Antonenko, E. A. Cherepanov, A. K. Nasirov, V. B. Permjakov, and V. V. Volkov, Phys. Lett. B **319**, 425 (1993); Phys. Rev. C **51**, 2635 (1995); G. G. Adamian, N. V. Antonenko, and W. Scheid, Nucl. Phys. **A618**, 176 (1997); G. G. Adamian, N. V. Antonenko, W. Scheid, and V. V. Volkov, *ibid.* **A627**, 361 (1997).

[6] G. G. Adamian, N. V. Antonenko, W. Scheid, and V. V. Volkov, Nucl. Phys. **A633**, 409 (1998); Nuovo Cimento A **110**, 1143 (1997).

[7] G. G. Adamian, N. V. Antonenko, and W. Scheid, Nucl. Phys. **A678**, 24 (2000).

[8] R. V. Jolos, A. K. Nasirov, and A. I. Muminov, Eur. Phys. J. A **4**, 245 (1999).

[9] E. A. Cherepanov, Report No. JINR, E7-99-27, 1999.

[10] B. Heusch *et al.*, Z. Phys. A **288**, 391 (1978); C. Lebrun *et al.*, Nucl. Phys. **A321**, 207 (1979); B. Borderie *et al.*, Z. Phys. A **299**, 263 (1981); B. B. Back *et al.*, Phys. Rev. Lett. **46**, 1068 (1981); **50**, 818 (1983); R. Bock *et al.*, Nucl. Phys. **A388**, 334 (1982); M. B. Tsang *et al.*, Phys. Lett. **129B**, 18 (1983); Z. Zheng *et al.*, Nucl. Phys. **A422**, 447 (1984); G. Guarino *et al.*, *ibid.* **A424**, 157 (1984); J. Toke *et al.*, *ibid.* **A440**, 327 (1985).

[11] W. Q. Shen *et al.*, Phys. Rev. C **36**, 115 (1987).

[12] M. G. Itkis *et al.*, *7th International Conference on Clustering Aspects of Nuclear Structure and Dynamics* (World Scientific, Singapore, 2000), p. 386.

[13] Ch. Ngo, Prog. Part. Nucl. Phys. **16**, 139 (1986).

[14] G. G. Adamian, A. K. Nasirov, N. V. Antonenko, and R. V. Jolos, Fiz. Elem. Chastits At. Yadra **25**, 1379 (1994) [Phys. Part. Nucl. **25**, 583 (1994)].

[15] W. U. Schröder and J. R. Huizenga, in *Treatise on Heavy-Ion Science*, edited by D. A. Bromley (Plenum, New York, 1984), Vol. 2, p. 115.

[16] W. von Oertzen, Z. Phys. A **342**, 177 (1992).

[17] L. G. Moretto and J. S. Sventek, Phys. Lett. **58B**, 26 (1975).

[18] G. G. Adamian, N. V. Antonenko, R. V. Jolos, and A. K. Nasirov, Nucl. Phys. **A551**, 321 (1993).

[19] N. V. Antonenko and R. V. Jolos, Yad. Fiz. **50**, 98 (1989).

[20] Yu. F. Smirnov and Yu. M. Tchuvil'sky, Phys. Lett. **134B**, 25 (1984); O. F. Nemetz, V. G. Neudatchin, A. T. Rudchik, Yu. F. Smirnov, and Yu. M. Tchuvil'sky, *Nucleonic Clusters in Nuclei and the Many-Nucleon Transfer Reactions* (Naukova Dumka, Kiev, 1988).

[21] G. G. Adamian, N. V. Antonenko, and Yu. M. Tchulvil'sky, Phys. Lett. B **451**, 289 (1999).

[22] G. G. Adamian, N. V. Antonenko, S. P. Ivanova, and W. Scheid, Nucl. Phys. **A646**, 29 (1999).

[23] A. Diaz-Torres, N. V. Antonenko, and W. Scheid, Nucl. Phys. **A652**, 61 (1999).

[24] A. Diaz-Torres, G. G. Adamian, N. V. Antonenko, and W. Scheid, Phys. Lett. B **481**, 228 (2000).

[25] G. G. Adamian, N. V. Antonenko, A. Diaz-Torres, and W. Scheid, Nucl. Phys. **A671**, 233 (2000).

[26] G. G. Adamian, R. V. Jolos, and A. K. Nasirov, Yad. Fiz. **55**, 660 (1992).

[27] V. G. Solovev, *Theory of Complex Nuclei* (Nauka, Moscow, 1971); V. A. Chepurnov, Yad. Fiz. **6**, 955 (1967).

[28] A. Diaz-Torres, G. G. Adamian, N. V. Antonenko, and W. Scheid, Nucl. Phys. **A679**, 410 (2001).

[29] M. Abramovitz and J. A. Stegun, *Handbook of Mathematical Functions* (Nauka, Moscow, 1979), p. 254.

[30] N. V. Antonenko, S. P. Ivanova, R. V. Jolos, and W. Scheid, Phys. Rev. C **50**, 2063 (1994); N. V. Antonenko and R. V. Jolos, Z. Phys. A **341**, 459 (1992).

[31] P. Gippner *et al.*, Phys. Lett. B **252**, 198 (1990).

[32] A. K. Nasirov *et al.*, Proceedings of XIV International Workshop on Nuclear Fission Physics (Obninsk, in press).

[33] H. A. Kramers, Physica (Amsterdam) **4**, 284 (1940); V. M. Strutinsky, Phys. Lett. **47B**, 121 (1973).

[34] P. Grangé *et al.*, Phys. Rev. C **27**, 2063 (1983); P. Grangé, Nucl. Phys. **A428**, 37c (1984).

[35] P. Fröbrich and G. R. Tillack, Nucl. Phys. **A540**, 353 (1992).

[36] G. G. Adamian, N. V. Antonenko, and R. V. Jolos, Nucl. Phys. **A584**, 205 (1995).

[37] I. I. Gonchar and G. I. Kosenko, Yad. Fiz. **53**, 133 (1991).

[38] R. V. Jolos, S. M. Lukyanov, A. K. Nasirov, V. P. Permjakov, V. S. Salamatin, and G. G. Chubarian, Yad. Fiz. **50**, 239 (1989).

[39] D. J. Hinde, D. Hilscher, and H. Rossner, Nucl. Phys. **A502**, 497c (1989).

[40] H. Gäggeler *et al.*, Z. Phys. A **316**, 291 (1984).

[41] A. B. Quint *et al.*, Z. Phys. A **346**, 119 (1993).

[42] V. E. Viola, Nucl. Data, Sect. A **1**, 391 (1966); V. E. Viola, K. Kwiatkowski, and M. Wolker, Phys. Rev. C **31**, 1550 (1985).